

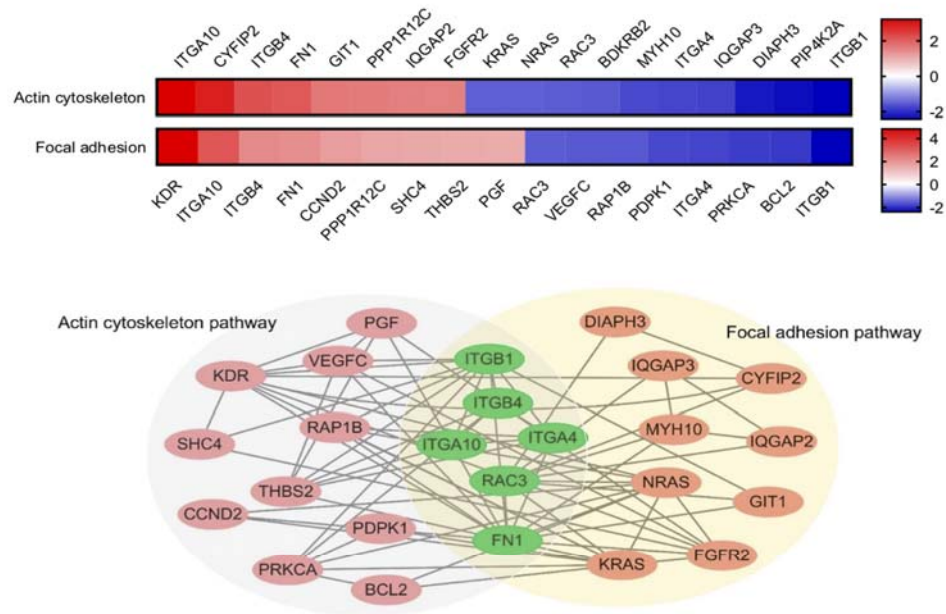
Supplemental Materials

Molecular Biology of the Cell

Na *et al.*

Supplementary materials

A



B

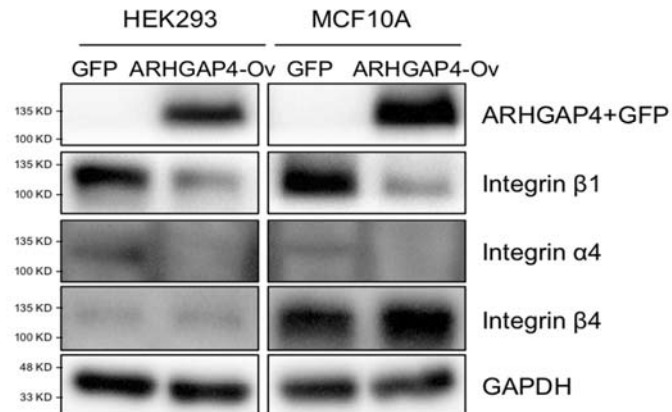


Figure S1. (A) Specific DEGs detected in “actin cytoskeleton” and “focal adhesion” categories, with their ARHGAP4/EGFP fold changes in red (upregulation) and blue (downregulation) color (upper) and with their mutual relationship in a Venn diagram (lower). Mutual relationships are comprised of known relationships provided by the database, and the connection between each of the related two genes are indicated by the lines. Among them, 6 DEGs (green) are shared by the two categories. (B) Immunoblots showing the expression of integrin molecules in HEK293 and MCF10A cells with (ARHGAP4-Ov) or without (GFP) ARHGAP4 overexpression.

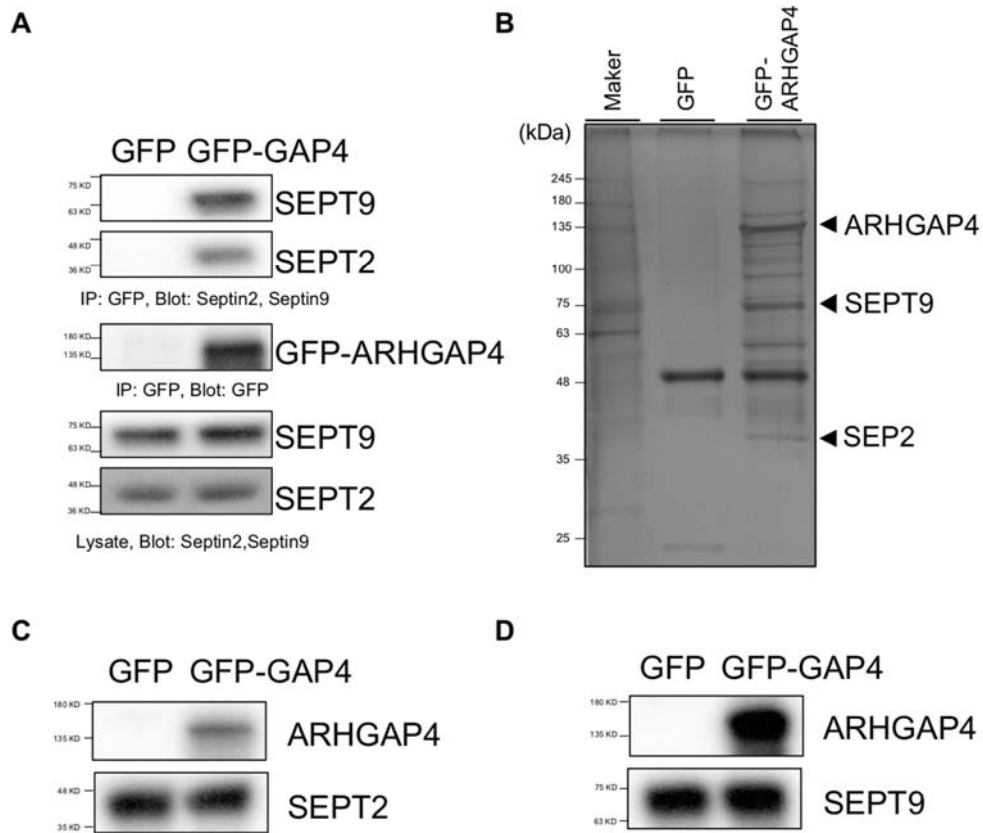


Figure S2. (A) MCF10A cells expressing EGFP or EGFP-ARHGAP4 were extracted and analyzed for immunoprecipitation with magnetic beads conjugated with an equal GFP antibody. (B) Immunoprecipitates and interacting proteins were stained by Silver Stain MS Kit (Wako). Coimmunoprecipitation shows that ARHGAP4 was pulled down with GFP-tagged SEPT2 and SEPT9, but not with GFP protein in MCF10A cells. (C) SEPT2 enables pull-down of GFP-tagged ARHGAP4, but not GFP. (D) SEPT9 enables pull-down of GFP-tagged ARHGAP4, but not GFP.

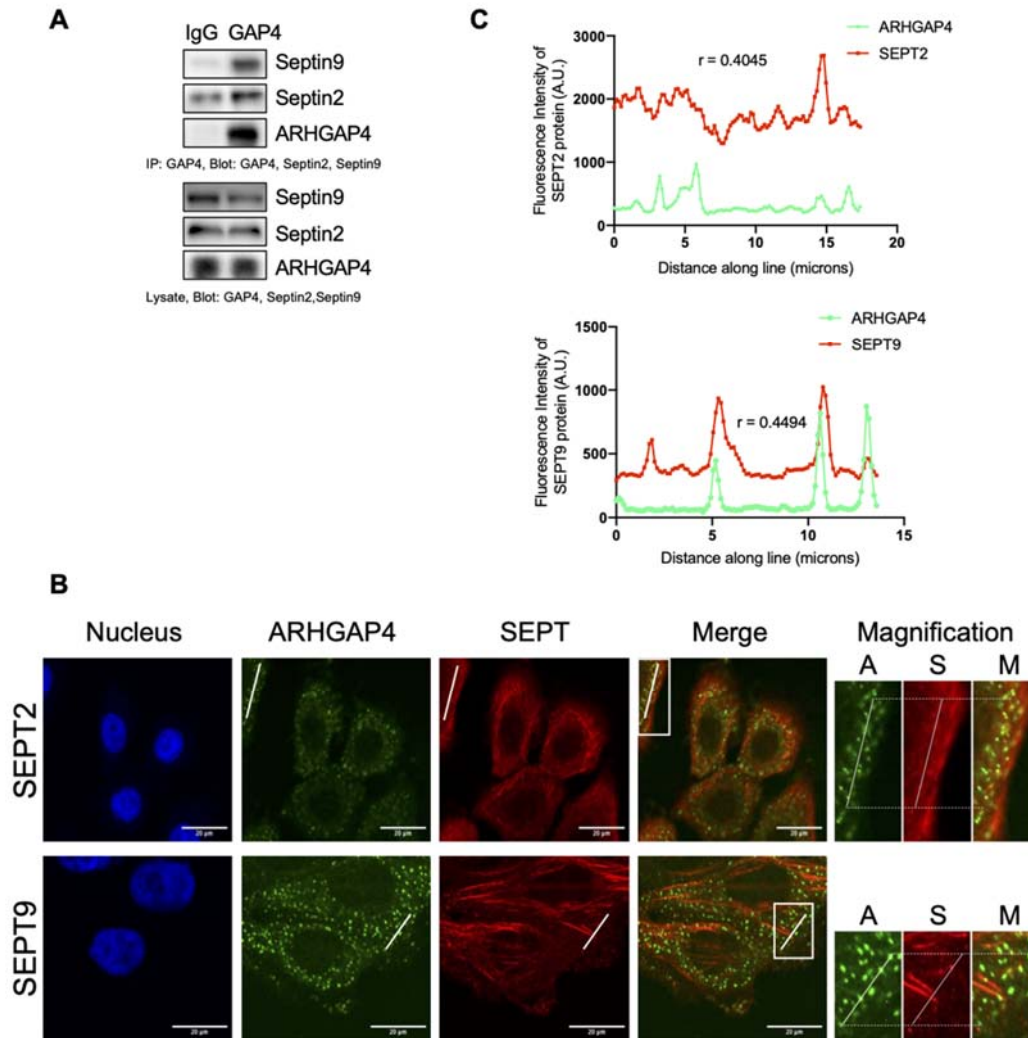


Figure S3. (A) BXPC3 cells were extracted and analyzed for immunoprecipitation with magnetic beads conjugated with an equal ARHGAP4 antibody. (B) Immunofluorescence shows colocalization of ARHGAP4, SEPT2, and SEPT9 in BXPC3 cells. Magnified views of the white rectangular regions in Merge are shown on the right panel, in which A, S, and M stand for ARHGAP4, SEPT, and Merge, respectively. The both ends of the survey line are connected by the dotted lines in Magnification. Note that the survey line is omitted in M to show the uncropped images. (C) Intensity distribution along the length of the white lines in B, showing ARHGAP4 (green) and SEPT2 (upper, red) or SEPT9 (lower, red) with an r representing the Pearson correlation coefficient. Scale, 20 μ m.

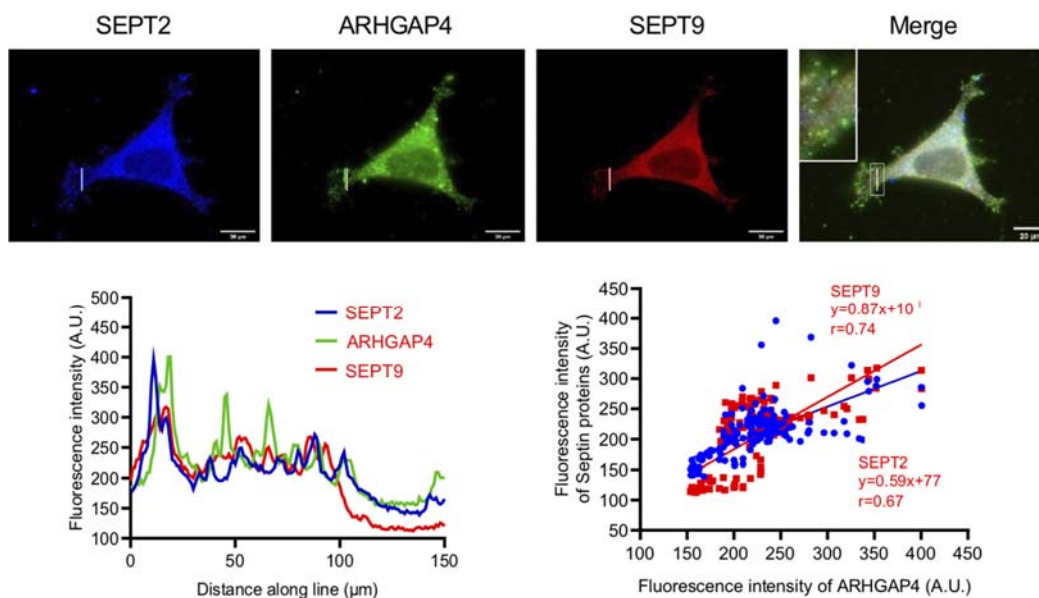
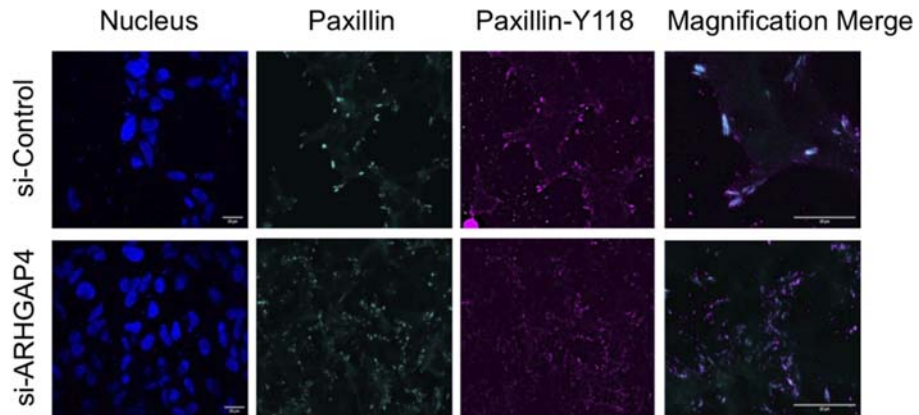


Figure S4. Confocal microscopic images of Immunofluorescence shows colocalization of ARHGAP4, SEPT2, and SEPT9 in HEK293 cells. The lower graphs show the relationship of the intensity of each protein along the line shown in the upper images, in which the regression lines were determined by the least-squares method with an r representing the Pearson correlation coefficient. Scale, 20 μm .

A



B

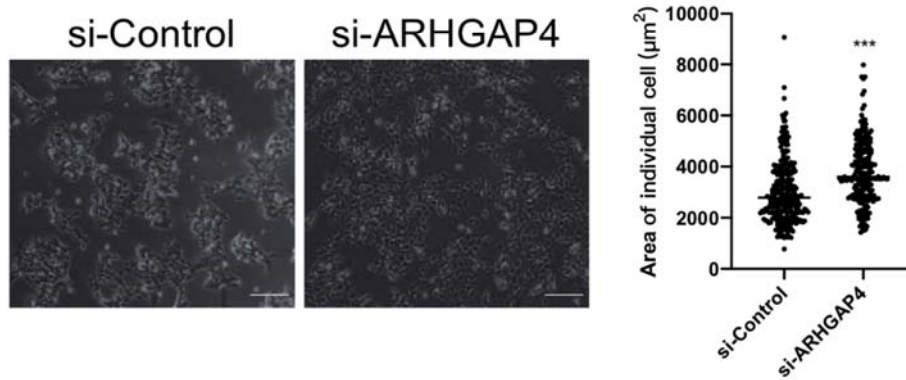


Figure S5. (A) Immunofluorescence of paxillin and paxillin-Y118 to observe the effect of ARHGAP4 depletion on FAs compared to control. Scale, 25 μm . (B) Bright-field of HEK293 cells treated with si-Control or si-ARHGAP4. Plots of individual cell area. Scale, 5 mm.

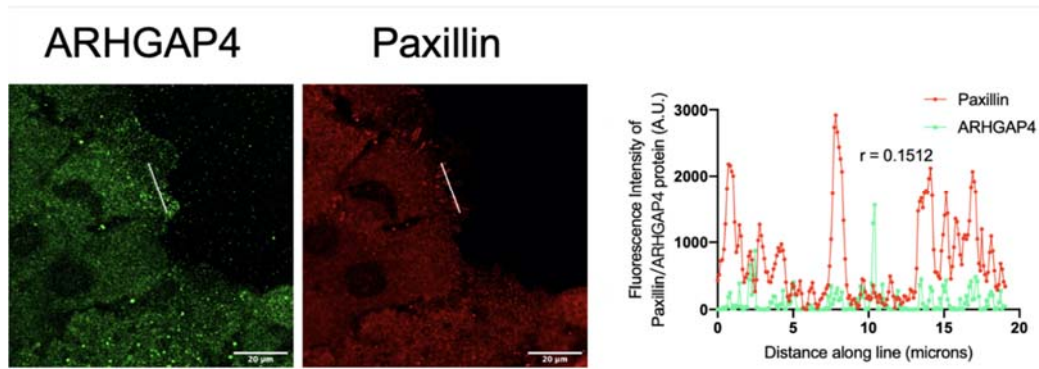


Figure S6. Immunofluorescence of ARHGAP4 and paxillin in Bxpc3 cells suggests that there is no obvious colocalization between them. The right graph shows the intensity distribution along the length of the white lines in the left images, showing ARHGAP4 (green) and paxillin (red) with an r representing the Pearson correlation coefficient Scale, 20 μ m.

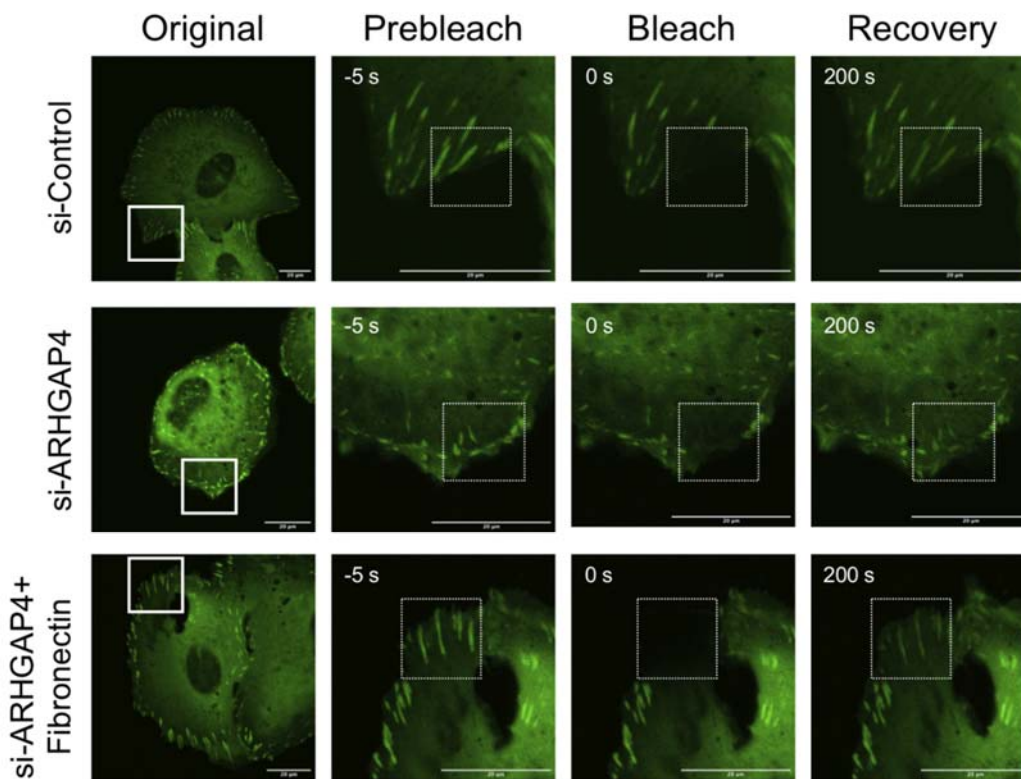


Figure. S7. Fluorescence images of EGFP-vinculin during the FRAP experiments

performed on control cells, ARHAGP4-depletion cells, and ARHAGP4-depletion cells with fibronectin coating. The white boxes in the images at Original are magnified on the right. The areas with the dotted white boxes were photobleached (time = 0 second), which partly recovered in fluorescence intensity at time = 200 seconds. The time evolution (Figure 3F) was analyzed to determine the extent of the recovery related to the stability of the FAs (Figure 3G). Scale, 20 μ m.

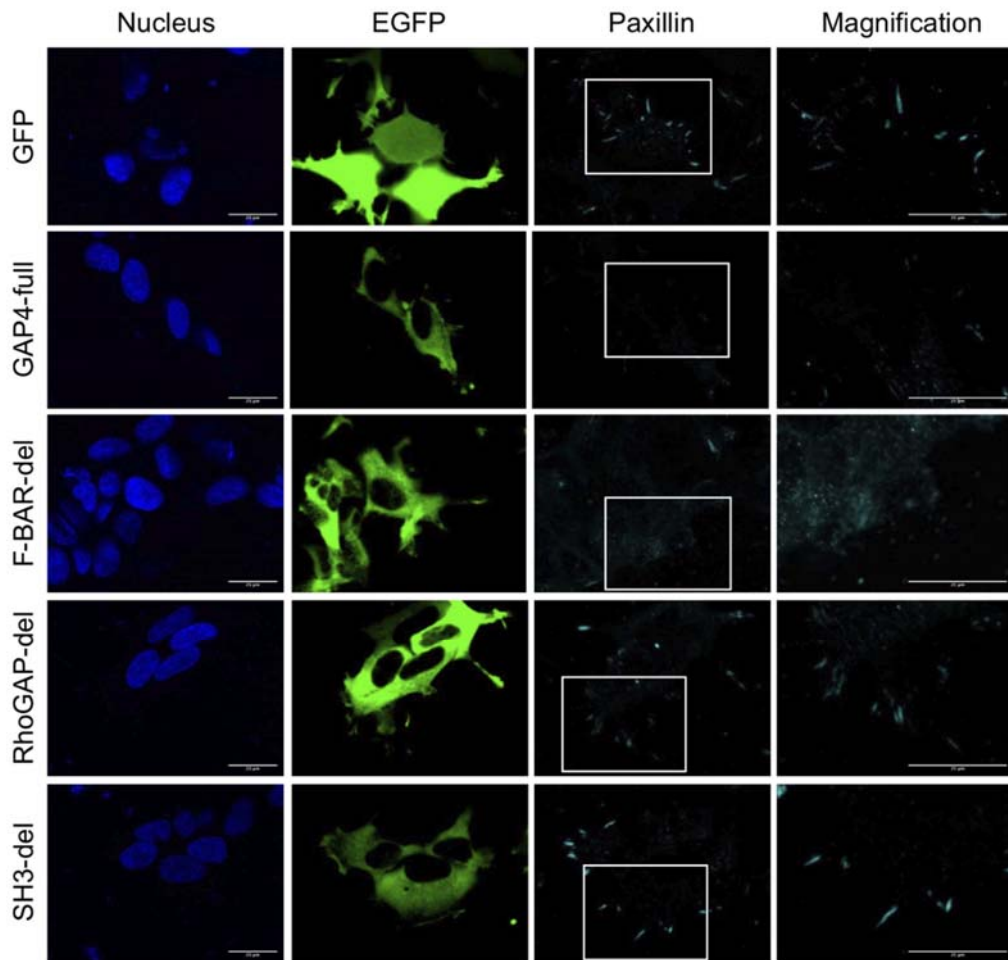


Figure. S8. Immunofluorescence of cells expressing GFP or the mutants described. The boxes in the paxillin images are magnified in the right columns. Scale, 25 μ m.

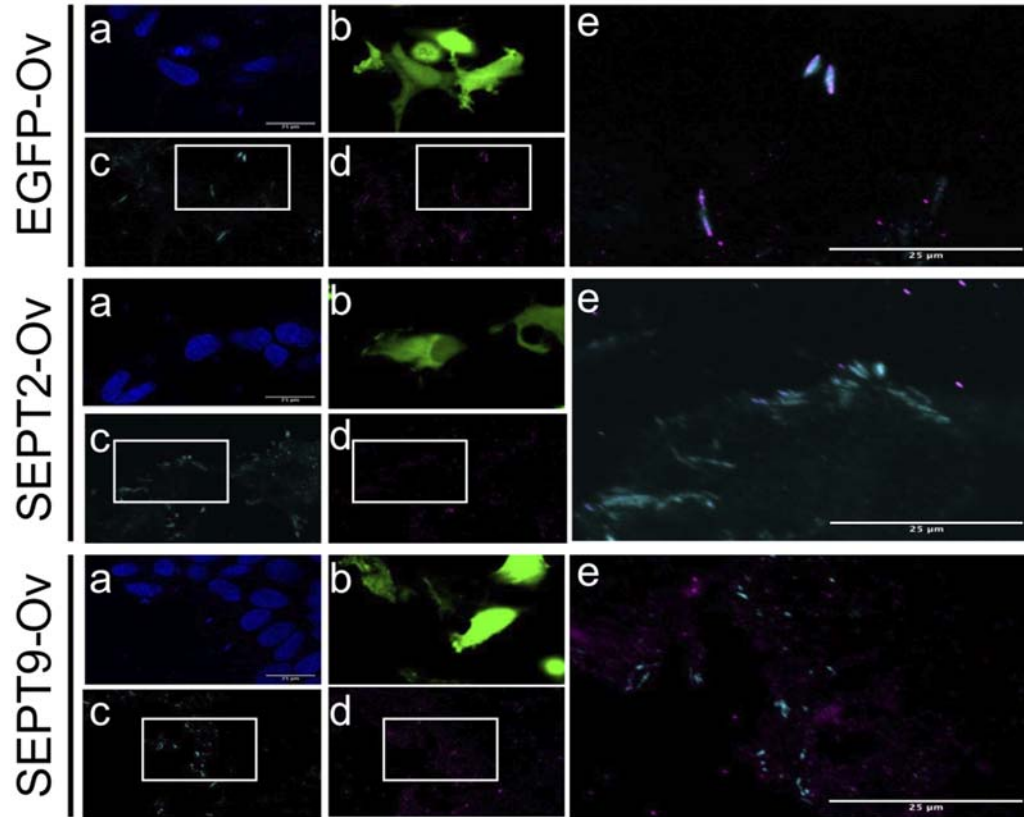


Figure S9. Immunofluorescence of cells overexpressed with EGFP, EGFP-labeled SEPT2, or EGFP-labeled SEPT9 shows the nucleus (a), EGFP (b), paxillin (c), paxillin-Y118 (d), and merge magnification of paxillin and paxillin-Y118 (e). Scale, 25 μ m.

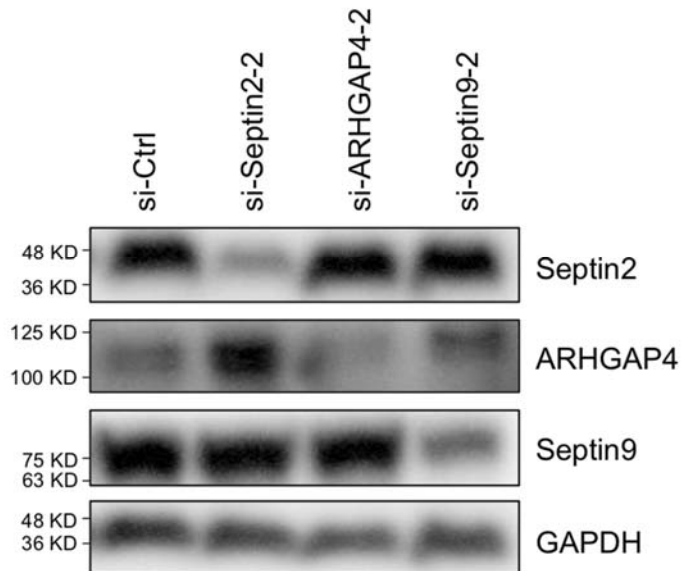


Figure S10. Immunoblots show that SEPT2 and SEPT9 depletion upregulates ARHGAP4 expression; meanwhile, ARHGAP4 depletion does not affect SEPT2 and SEPT9. The siRNAs for this figure are different with those of Figure 6A.

Table S1. The DEGs caused by ARHGAP4.

Table S2. The DEGs in “cytoskeleton” and “focal adhesion” pathway.

Table S3. The primer sequences used to construct the plasmids.

Table S4. The siRNA sequences.

Table S5. The antibodies used in this study.

Table S1 The DEGs caused by ARHGAP4 (Fold change > 1.5)			
Gene Symbol	Gene ID	N EGFP	N GAP4
ZZZ3	26009	7.005300	6.745060
ZZEF1	23140	6.257500	6.305360
ZYX	7791	7.298810	7.405070
ZYG11B	79699	7.695230	7.389130
ZYG11A	440590	2.273910	2.364040
ZXDC	79364	5.443190	5.650680
ZXDB	158586	4.861100	5.522130
ZXDA	7789	2.374260	2.374260
ZWINT	11130	6.058510	6.306430
ZWILCH	55055	7.600110	7.230580
ZW10	9183	6.788850	6.314760
ZUFSP	221302	4.398270	3.699020
ZSWIM8-AS1	100507331	3.739100	3.981370
ZSWIM8	23053	5.235050	5.759950
ZSWIM7	125150	3.944600	3.944600
ZSWIM6	57688	6.523100	6.846710
ZSWIM5	57643	4.197910	3.305620
ZSWIM4	65249	4.526510	4.814170
ZSWIM3	140831	3.488470	3.219190
ZSWIM2	151112	1.603330	1.872180
ZSWIM1	90204	6.241020	6.312010
ZSCAN9	7746	3.950330	3.786500
ZSCAN5CP	649137	2.393100	2.475050
ZSCAN5B	342933	1.941610	1.803550
ZSCAN5A	79149	5.265820	5.703880
ZSCAN4	201516	1.982880	1.907180
ZSCAN32	54925	5.384820	5.653330
ZSCAN31	64288	2.643080	2.785490
ZSCAN30	100101467	3.806040	3.770210
ZSCAN29	146050	5.789390	5.913420
ZSCAN26	7741	4.312510	4.228530
ZSCAN25	221785	4.878110	4.715910
ZSCAN23	222696	2.880910	3.364700
ZSCAN22	342945	5.527550	5.732880
ZSCAN21	7589	5.979200	5.963560
ZSCAN20	7579	4.336440	4.381650
ZSCAN2	54993	3.999520	4.201790
ZSCAN18	65982	3.784170	3.692270
ZSCAN16-AS1	100129195	3.127560	3.385490
ZSCAN16	80345	3.301000	3.478920
ZSCAN12P1	221584	4.044050	4.150050
ZSCAN12	9753	3.863210	2.973970
ZSCAN10	84891	3.943350	4.177670
ZSCAN1	284312	4.155140	4.610530

Table S2 The DEGs in “cytoskeleton” and “focal adhesion” pathway

	Aliases for KDR Gene	ARHGAP4/EGFP Fold change	The function of cellular processes				Representative References
			Cancer-related	Movement-related	Proliferation-related	Cytoskeleton-related	
KDR	Kinase Insert Domain Receptor, Vascular Endothelial Growth Factor Receptor 2, VEGFR, FLK1	4.831496	O	O	O	O	1. VEGFR2 and VEGF-C Suppresses the Epithelial-Mesenchymal Transition Via YAP in Retinal Pigment Epithelial Cells. Y. Du et al. Current Molecular Medicine, 2018 2. Vascular Endothelial Growth Factor Regulates Focal Adhesion Assembly in Human Brain Microvascular Endothelial Cells Through Activation of the Focal Adhesion Kinase and Related Adhesion Focal Tyrosine Kinase. Hava Karsenty Avraham et al. J Biol Chem, 2003 3. Apatinib Affect VEGF-mediated Cell Proliferation, Migration, Invasion via Blocking VEGFR2/RAF/MEK/ERK and PI3K/AKT Pathways in Cholangiocarcinoma Cell, Manping Huang et al. BMC Gastroenterol, 2018
ITGA10	Integrin Subunit Alpha 10	3.219798	X	O	O	O	1. Integrin-α10 Dependency Identifies RAC and RICTOR as Therapeutic Targets in High-Grade Myxofibrosarcoma, Tomoyo Okada et al, Cancer Discov, 2016 2. Prednisolone Induces Osteoporosis-Like Phenotypes via Focal Adhesion Signaling Pathway in Zebrafish Larvae, Lei Huo et al, Biol Open, 2018 3. Integrin α10, a Novel Therapeutic Target in Glioblastoma, Regulates Cell Migration, Proliferation, and Survival, Matilda Munksgaard Thorén et al. Cancers, 2019
ITGB4	Integrin Subunit Beta 4	2.197114	O	O	O	O	1. ITGB4-mediated Metabolic Reprogramming of Cancer-Associated Fibroblasts, Jin Sol Sung et al. Oncogene, 2020 2. Activation of Focal Adhesion Kinase Through an Interaction With β4 Integrin Contributes to Tumorigenicity of Colon Cancer, Yu-Ling Tai et al. FEBS Lett. 2016 3. Deletion of TMEM268 Inhibits Growth of Gastric Cancer Cells by Downregulating the ITGB4 Signaling Pathway. Dubeiqi Hong et al. Cell Death Differ. 2019 4. Metallopanstimulin-1 Regulates Invasion and Migration of Gastric Cancer Cells Partially Through Integrin β4. Zhong yin Yang et al. Carcinogenesis. 2013
FN1	Fibronectin 1, Cold-Insoluble Globulin, Migration-Stimulating Factor	2.088750	O	O	O	O	1. Down-regulation of FN1 Inhibits Colorectal Carcinogenesis by Suppressing Proliferation, Migration, and Invasion, Xun Cai et al. J Cell Biochem. 2018 2. Fibronectin Is Up-Regulated in Podocytes by Mechanical Stress. Felix Kliewe et al. FASEB J. 2019 3. Fibronectin 1 Promotes Melanoma Proliferation and Metastasis by Inhibiting Apoptosis and Regulating EMT. Bifei Li et al. Onco Targets Ther. 2019 4. Fibronectin promotes cervical cancer tumorigenesis through activating FAK signaling pathway. Yuzhen Zhou et al. J Cell Biochem
CCND2	Cyclin D2, G1/S-Specific Cyclin-D2, MPPH3	1.794610	O	O	O	O	1. Long noncoding RNA FOXD2-AS1 promotes glioma malignancy and tumorigenesis via targeting miR-185-5p/CCND2 axis. Shen F et al. J Cell Biochem. 2019 2. miR-198 Represses the Proliferation of HaCaT Cells by Targeting Cyclin D2. Jian Wang et al. Int J Mol Sci. 2015 3. Loss of a negative feedback loop involving pea3 and cyclin d2 is required for pea3-induced migration in transformed mammary epithelial cells. Ladam F et al. Mol Cancer Res. 2013
PPP1R12C	Protein Phosphatase 1 Regulatory Subunit 12C, Myosin-Binding Subunit 85, P85, Leukocyte Receptor Cluster (LRC) Member 3, AAVS1	1.648496	O	X	X	O	1. Identification of Tumor-Educated Platelet Biomarkers of Non-Small-Cell Lung Cancer. Meiling Sheng et al. Onco Targets Ther. 2018 2. Novel roles for scleraxis in regulating adult tenocyte function. Anne E.C et al. BMC Cell Biology. 2018 3. Altered Expression of Human Smooth Muscle Myosin Phosphatase Targeting (MYPT) Isovariants With Pregnancy and Labor. Jon Lartey et al. Plos One. 2016
SHC4	SHC Adaptor Protein 4, Rai-Like Protein, SHCD	1.592839	O	O	O	O	1. The ShcD Signaling Adaptor Facilitates Ligand-Independent Phosphorylation of the EGF Receptor, Melanie K B Wills et al. Mol Biol Cell. 2014 2. Role of TGF-β in the Motility of ShcD-overexpressing 293 Cells. Sara Amer et al. Mol Med Rep. 2019 3. Cellular Heterogeneity During Embryonic Stem Cell Differentiation to Epiblast Stem Cells Is Revealed by the ShcD/RaLP Adaptor Protein, Margherita Y Turcoet al. Stem Cells. 2012 4. Signaling adaptor ShcD suppresses extracellular signal-regulated kinase (Erk) phosphorylation distal to the Ret and Trk neurotrophic receptors. Wills MK et al. J Biol Chem. 2017
THBS2	Thrombospondin 2, TSP2	1.582406	O	O	O	O	1. THBS2 is a biomarker for AJCC stages and a strong prognostic indicator in colorectal cancer. Tian Q et al. J BUON. 2018 2. Silencing of COL1A2, COL6A3, and THBS2 inhibits gastric cancer cell proliferation, migration, and invasion while promoting apoptosis through the PI3k-Akt signaling pathway. Ao R et al. J Cell Biochem. 2018 3. Transcriptomic profile reveals molecular events associated to focal adhesion and invasion in canine mammary gland tumour cell lines. Cordeiro YG et al. Vet Comp Oncol.
PGF	Placental Growth Factor, PGFL, PIGF	1.541121	O	O	O	O	1. Placental growth factor promotes epithelial-mesenchymal transition-like changes in ARPE-19 cells under hypoxia. Zhang Y et al. Mol Vis. 2018 2. PIGF Knockdown Inhibited Tumor Survival and Migration in Gastric Cancer Cell via PI3K/Akt and p38MAPK Pathways. Hassan Akrami et al. Cell Biochem Funct. 2016
RAC3	Rac Family Small GTPase 3, Ras-Related C3 Botulinum Toxin Substrate 3, P21-Rac3, Rho Family, Small GTP Binding Protein Rac3	-1.523997	O	O	O	O	1. Rac3 Regulates Cell Invasion, Migration and EMT in Lung Adenocarcinoma through p38 MAPK Pathway. Zhang C et al. J Cancer. 2017 2. Rac function is crucial for cell migration but is not required for spreading and focal adhesion formation. Steffen A et al. J Cell Sci. 2013 3. Rac3 regulates breast cancer invasion and metastasis by controlling adhesion and matrix degradation. Donnelly SK et al. J Cell Biol. 2017
VEGFC	Flt4-L, Vascular Endothelial Growth Factor C,VRP, LMPH1D	-1.585403	O	O	O	O	1. Suppression of Vascular Endothelial Growth Factor Receptor 3 (VEGFR3) and Vascular Endothelial Growth Factor C (VEGFC) Inhibits Hypoxia-Induced Lymph Node Metastases in Cervix Cancer. Naz Chaudary et al. Gynecol Oncol. 2011 2. VEGFC acts as a double-edged sword in renal cell carcinoma aggressiveness. Ndiaye PD et al. Theranostics. 2019

RAP1B	GTP-Binding Protein Smg P21B, Ras Family Small GTP Binding Protein RAP1B, RAS-Related Protein RAP1B, K-REV	-1.587152	○	○	○	○	<p>1. Rap1b enhances the invasion and migration of hepatocellular carcinoma cells by up-regulating Twist 1. Tang Z et al. Exp Cell Res. 2018</p> <p>2. Rap1b Promotes Notch-Signal-Mediated Hematopoietic Stem Cell Development by Enhancing Integrin-Mediated Cell Adhesion. Rho SS et al. Dev Cell. 2019</p>
PDPK1	3-Phosphoinositide Dependent Protein Kinase 1, PkB Kinase Like Gene 1, PDPK2P, PDPK2, HPDK1	-1.741137	○	○	○	○	<p>1. miR-16-2-3p inhibits cell proliferation and migration and induces apoptosis by targeting PDPK1 in maxillary primordium mesenchymal cells. Han T et al. Int J Mol Med. 2019.</p> <p>2. PDK1 induces JunB, EMT, cell migration and invasion in human gallbladder cancer. Lian S et al. Oncotarget. 2015</p> <p>3. Serine/Threonine Kinase 3-Phosphoinositide-Dependent Protein Kinase-1 (PDK1) as a Key Regulator of Cell Migration and Cancer Dissemination. Di Blasio L et al. Cancers. 2017</p>
ITGA4	Integrin Subunit Alpha 4, CD49D, Antigen CD49D, Alpha-4 Subunit Of VLA-4 Receptor	-1.767046	○	○	○	○	<p>1. MiR-30s Family Inhibit the Proliferation and Apoptosis in Human Coronary Artery Endothelial Cells Through Targeting the 3'UTR Region of ITGA4 and PLCG1. Ma F et al. J Cardiovasc Pharmacol. 2016</p> <p>2. Methionine and choline supply during the peripartal period alter polymorphonuclear leukocyte immune response and immunometabolic gene expression in Holstein cows. Zhou Z et al. J Dairy Sci. 2018</p>
PRKCA	Protein Kinase C Alpha, Aging-Associated Gene 6, PRKACA, AAG6	-1.848276	○	○	○	○	<p>1. A recurrent point mutation in PRKCA is a hallmark of chordoid gliomas. Rosenberg S et al. Nat Commun. 2018</p> <p>2. Inhibition of ZL55 cell proliferation by ADP via PKC-dependent signalling pathway. Muscella A et al. J Cell Physiol. 2018</p> <p>3. Protein kinase C α enhances migration of breast cancer cells through FOXC2-mediated repression of p120-catenin. Pham TND et al. BMC Cancer. 2017</p>
BCL2	BCL2 Apoptosis Regulator, Protein Phosphatase 1, Regulatory Subunit 50, PPP1R50	-1.889455	○	○	○	○	<p>1. Regulating the BCL2 Family to Improve Sensitivity to Microtubule Targeting Agents. Whitaker RH et al. Cells. 2019</p> <p>2. miR-34a targets BCL-2 to suppress the migration and invasion of sinonasal squamous cell carcinoma. Zhao Y et al. Oncol Lett. 2018</p> <p>3. BCL-2: Long and winding path from discovery to therapeutic target. Schenk RL et al. Biochem Biophys Res Commun. 2017</p>
ITGB1	Integrin Subunit Beta 1, Glycoprotein Iia, MSK12, GPIIA, FNRB, MDF2, VLA-4 Subunit Beta, CD29	-2.394791	○	○	○	○	<p>1. β1 integrin signaling promotes neuronal migration along vascular scaffolds in the post-stroke brain. Fujioka T et al. EBioMedicine. 2017</p> <p>2. Integrin-β1 regulates chondrocyte proliferation and apoptosis through the upregulation of GIT1 expression. Zhang LQ et al. Int J Mol Med. 2015</p> <p>3. CD93 promotes β1 integrin activation and fibronectin fibrillogenesis during tumor angiogenesis. Lugano R et al. J Clin Invest. 2018</p>
CYFIP2	Cytoplasmic FMR1 Interacting Protein 2, P53-Inducible Protein 121, PIR121, EIEE65	2.907441	○	○	○	○	<p>1. Inhibition of CYFIP2 promotes gastric cancer cell proliferation and chemoresistance to 5-fluorouracil through activation of the Akt signaling pathway. Jiao S et al. Oncol Lett. 2017</p> <p>2. PIR121 regulates pseudopod dynamics and SCAR activity in Dictyostelium. Blagg S et al. Curr Biol. 2003</p> <p>3. Distinct Interaction Sites of Rac GTPase with WAVE Regulatory Complex Have Non-redundant Functions in Vivo. MatthiasSchaks et al. Curr Biol. 2018</p>
GIT1	GIT ArfGAP 1, ARF GTPase-Activating Protein GIT1, G Protein-Coupled Receptor Kinase-Interactor 1	1.674546	○	○	○	○	<p>1. Inhibiting GIT1 reduces the growth, invasion, and angiogenesis of osteosarcoma. Zhang Z et al. Cancer Manag Res. 2018</p> <p>2. Periodic Mechanical Stress Stimulates GIT1-Dependent Mitogenic Signals in Rat Chondrocytes Through ERK1/2 Activity. Ren K et al. Cell Physiol Biochem. 2018</p> <p>3. MiR-138 inhibits cell proliferation and reverses epithelial-mesenchymal transition in non-small cell lung cancer cells by targeting GIT1 and SEMA4C. Li J et al. J Cell Mol Med. 2015</p>
IQGAP2	IQ Motif Containing GTPase Activating Protein 2, Ras GTPase-Activating-Like Protein IQGAP2	1.586580	○	○	○	○	<p>1. Epigenetic regulation of IQGAP2 promotes ovarian cancer progression via activating Wnt/β-catenin signaling. Deng Z et al. Int J Oncol. 2016</p> <p>2. IQGAP2 Inhibits Migration and Invasion of Gastric Cancer Cells via Elevating SHIP2 Phosphatase Activity. Xu L et al. Int J Mol Sci. 2020</p> <p>3. IQGAP2, A candidate tumour suppressor of prostate tumorigenesis. Xie Y et al. Biochim Biophys Acta. 2012</p> <p>4. IQGAP2 functions as a GTP-dependent effector protein in thrombin-induced platelet cytoskeletal reorganization. Schmidt VA et al. Blood, 2003</p>
FGFR2	Fibroblast Growth Factor Receptor 2, KGFR, Jackson-Weiss Syndrome, Keratinocyte Growth Factor Receptor	1.568266	○	○	○	○	<p>1. Cancer Mutations in FGFR2 Prevent a Negative Feedback Loop Mediated by the ERK1/2 Pathway. Szybowska P et al. Cells. 2019</p> <p>2. FGFR2-activating mutations disrupt cell polarity to potentiate migration and invasion in endometrial cancer cell models. Stehbins SJ et al. J Cell Sci. 2018</p> <p>3. FGF9/FGFR2 increase cell proliferation by activating ERK1/2, Rb/E2F1, and cell cycle pathways in mouse Leydig tumor cells. Chang MM et al. Cancer Sci. 2018</p>
KRAS	KRAS Proto-Oncogene, GTPase, Cellular Transforming Proto-Oncogene, PR310 C-K-Ras Oncogene, Transforming Protein P21, K-Ras P21 Protein	-1.503141	○	○	○	○	<p>1. Cancer cell-autonomous TRAIL-R signaling promotes KRAS-driven cancer progression, invasion, and metastasis. von Karstedt S et al. Cancer Cell. 2015</p> <p>2. Effects of PTEN Loss and Activated KRAS Overexpression on Mechanical Properties of Breast Epithelial Cells. Linthicum W et al. Int J Mol Sci. 2018</p>
NRAS	NRAS Proto-Oncogene, GTPase, V-Ras Neuroblastoma RAS Viral Oncogene Homolog, N-Ras Protein Part 4, CMNS	-1.511321	○	○	○	○	<p>1. Effects of miR-145-5p through NRAS on the cell proliferation, apoptosis, migration, and invasion in melanoma by inhibiting MAPK and PI3K/AKT pathways. Liu S et al. Cancer Med. 2017</p> <p>2. Mechanisms of Regulation of Pseudopodial Activity by the Microtubule System. A D Bershadsky et al. Symp Soc Exp Biol. 1993</p>
BDKRB2	Bradykinin Receptor B2, BK-2 Receptor, BKR2	-1.574823	○	○	○	○	<p>1. IRX1 influences peritoneal spreading and metastasis via inhibiting BDKRB2-dependent neovascularization on gastric cancer. Jiang J et al. Oncogene. 2011</p> <p>2. Serum bradykinin levels as a diagnostic marker in cervical cancer with a potential mechanism to promote VEGF expression via BDKRB2. Zhou Y et al. Int J Oncol. 2019</p>
MYH10	Myosin Heavy Chain 10, Nonmuscle Myosin Heavy Chain IIB, Cellular Myosin Heavy Chain, Type B	-1.723702	○	○	○	○	<p>1. Myosin Heavy Chain 10 (MYH10) Gene Silencing Reduces Cell Migration and Invasion in the Glioma Cell Lines U251, T98G, and SHG44 by Inhibiting the Wnt/β-Catenin Pathway. Wang Y et al. Med Sci Monit. 2018</p> <p>2. Mosaic loss of non-muscle myosin IIA and IIB is sufficient to induce mammary epithelial proliferation. Nguyen-Ngoc KV et al. J Cell Sci. 2017</p>

Table S3 The primer sequences are used to construct the plasmids

Gene name	Forward primers sequence 5'---> 3'	Reverse primers sequence 5'---> 3'
Septin2-plasmid construction	CGAATTCCATGTCTAAGCAACAGC	GCACAATTGCATTACACGTGGTGCCCGA
Septin9-plasmid construction	GCTGTACAAGATGAAGAAGTCTTACT	GCACAATTGCACACTACATCTCCGGGGCTT
ARHGAP4-plasmid construction	gtcgacggtaccgcgggcccATGGCCGCTCACGGGAAG	atctagatccggtggatcccTCAGTGTGGCTTGGGGGGTC

Table S4 The siRNA sequences

Gene Symbol	Full Gene Name	Company	Gene ID	siRNA ID	Sense siRNA Sequence	Antisense siRNA Sequence
ARHGAP4	Rho GTPase activating protein 4	Thermo Fisher Scientific	393	s1586	GUAUAACCAGAGACUCUUUtt	AAAGAGUCUCUGGUUAUACtg
	Rho GTPase activating protein 4	Thermo Fisher Scientific	393	s1587	ACCGAAACCUUCUACCUCAtt	UGAGGUAGAAGGUUUCGGUct
Septin2	Septin2	Thermo Fisher Scientific	4735	s9418	GCCUAUUCCUAACUGAUCUtt	AGAUCAGUUAGGAAUAGGCtg
	Septin2	Thermo Fisher Scientific	4735	s9419	GAAAUAUCGACUCUCAUAAAtt	UUUAUGAGAGUCGAUUUUCct
Septin9	Septin9	Thermo Fisher Scientific	10801	s21222	CGCACGAUAUUGAGGAGAAtt	UUCUCCUCAAUUCGUGCGtg
	Septin2	Thermo Fisher Scientific	10801	s21223	CAAUGACCAGUACGAGAAAtt	UUUCUCGUACUGGUCAUUGat

Table S5 The antibodies used in this study

Antibody	Company	Product code	Application/Concentration		
			IP	IF	WB
ARHGAP4	Proteintech	16697-1-AP		1:50	1:1000
ARHGAP4	Abcam	ab226835	2 µg/mg		1:2000
Septin2	Proteintech	11397-1-AP			1:1000
Septin2	Abcam	ab179436	2 µg/mg		1:2000
Septin9	Proteintech	10769-1-AP	2 µg/mg		1:1000
Paxillin	Abcam	ab32084		1:100	1:1000
FAK	BD Biosciences	610088		1:500	1:1000
Integrin β1	CST	#4706			1:1000
GAPDH	Wako	014-25524			1:5000
GFP	Wako	mFX73	2 µg/mg		
GFP	Wako	mFX75			1:1000
IgG	Wako	147-09521	2 µg/mg		